

Spiking Cerebellar Model with Multiple Plasticity Sites Reproduces Eye Blinking Classical Conditioning

Alberto Antonietti, Claudia Casellato, Jesus A. Garrido, Egidio D'Angelo, Alessandra Pedrocchi

Abstract — Eye blinking classical conditioning is one of the most extensively studied paradigms related to the cerebellum. In this work we have defined a realistic cerebellar model through the use of artificial spiking neural networks, testing it in computational simulations reproducing the eye blinking classical conditioning in multiple sessions of acquisition and extinction. We used two models: one with only the cortical plasticity and another with three plasticity sites, one plasticity at cortical level and two at nuclear level. We have compared the behavioral outcome of the two different models and proved that the model with a distributed plasticity produces a faster and more stable acquisition of conditioned responses in the re-acquisition phase with respect to the single plasticity model. This behavior is explained by the effect of the nuclear plasticities, which have a slow dynamics and can express memory consolidation and savings.

I. INTRODUCTION

The cerebellum is a fundamental processing unit for a large number of cognitive and motor tasks [1], one of the most studied paradigms in which the cerebellum is majorly involved is the Eye Blinking Classical Conditioning (EBCC) [2]. In the standard EBCC, a neutral Conditioned Stimulus (CS), e.g. a tone, precedes an attentive Unconditioned Stimulus (US), e.g. an electric stimulation of the periorbital area or an air-puff directed to the eye. The time interval between the onset of the CS and the onset of US is fixed and it is called Inter Stimulus Interval (ISI) [3]. At the beginning, the (animal or human) subjects show eyelid closures (blink) elicited by the US. After repeated presentations of CS and US paired during the acquisition phase, the subject learns to close his eyelids before the arrival of the US, this action is called Conditioned Response (CR). During the extinction phase, the subject continues to receive the CS only, without the presentation of US. At the beginning, the learned association leads to generate CRs still. At the end of the extinction phase, the subject does not show the previously acquired behavior.

Several studies proved the importance of the cerebellum for

the acquisition and extinction of CRs in EBCC sessions. The signal pathways which are involved during the EBCC are clear (see Fig. 1): the CS is conveyed from the Pontine Nuclei to the Granular Cells (GRs) through the Mossy Fibers (MFs); the US is conveyed from the Inferior Olive cells (IOs) to the Purkinje Cells (PCs) through the Climbing Fibers (CFs), PCs also receive excitatory synapses from GRs through the Parallel Fibers (PFs); the eyelid closure is commanded by the Deep Cerebellar Nuclei cells (DCNs) which excite the related motor neurons.

It is supposed that the learning capabilities of the cerebellum are related to the plasticity mechanisms which change the synaptic weights of the connections between different groups of cells. There are two well-known long term plasticities for the PF-PC connections: Long Term Potentiation (LTP) and Long Term Depression (LTD). They are assumed to be responsible of CR acquisition and extinction in EBCC protocol [4]. In the last years, other plasticity sites were hypothesized [5]–[7], both at cortical and nuclear level, in order to take into account the different time scales which can be identified in cerebellar adaptation. Specifically, the cerebellar learning can be separated into two components: a fast process related to the cortical plasticity and a slow process related to the nuclear plasticity.

The simplicity of the EBCC and the timing nature of the protocol led to use this paradigm as a test bench for computational models of the cerebellum, which range from simplified analog versions [3], [8], [9] to more realistic models using artificial Spiking Neural Networks (SNN) [10], [11]. Different models implement also different plasticity mechanisms, the majority takes into account the cortical plasticity only. In [11], a large-scale SNN (more than 100k neurons) was used in a robotic Pavlovian task, reproducing learning mechanisms with PF-PC plasticity. Very recently, Casellato et al. developed and tested a SNN-based cerebellar model in different tasks, such as EBCC and Vestibulo-Ocular Reflex both in computational simulations and embedded real robotic platforms [12]. This model has shown its effectiveness obtaining behaviors similar to neurophysiological experiments, exploiting only LTP and LTD plasticities at the PF-PC connections. Both Yamazaki and Casellato models did not implement nuclear plasticity mechanisms, in this work we aim to improve the second SNN model introducing two additional plasticities at the nuclear level, in particular LTP and LTD mechanisms at MF-DCN and PC-DCN synapses. We tested the models in computational simulations reproducing the EBCC protocol with two sessions, each made up of an acquisition phase and an extinction phase. Our aim is to highlight the behavioral differences between the SNN model equipped with the cortical plasticity only and with three plasticity sites. We

* This work was supported by grants of European Union: CEREBNET FP7-ITN238686, REALNET FP7-ICT270434, Human Brain Project HBP-604102

A. Antonietti C. Casellato and A. Pedrocchi are with the NeuroEngineering And medical Robotics Laboratory, Dept. Electronics, Information and Bioengineering, Politecnico di Milano, P.zza L. Da Vinci 32, 20133, Milano, Italy (telephone: +39-02-23999501 e-mail: alberto.antonietti@polimi.it).

J. A. Garrido is with the Dept. of Computer Architecture and Technology, University of Granada, Periodista Daniel Saucedo Arana, 18071, Granada, Spain.

E. D'Angelo is with the Brain Connectivity Center, IRCCS Istituto Neurologico Nazionale C. Mondino and the Dept. Brain and Behavioral Sciences, University of Pavia, Via Forlanini 6, 27100, Pavia, Italy.

expect that the addition of nuclear plasticities, which have a slow timescale, could introduce consolidation mechanisms, detectable mainly in the re-acquisition phase [13].

II. MATERIALS AND METHODS

A. Cerebellar topology

We started from a well-tested cerebellar model, exploiting the Event-Driven simulator based on Look-Up-Tables [14], a simulator of SNN which speeds up the simulation through the use of look-up-tables which reduces the computational load.

The SNN (Fig. 1) is composed of 100 MFs, which receive the CS, 2000 GRs, 24 IO, which receive the US, 24 PCs and 12 DCN, which produce the cerebellar output and therefore the CRs.

MFs are randomly connected with GRs, each GR receives 4 random connections, for a total of 8000 excitatory connections. The granular layer is a sparse representation of the input signal, due to the sparse coding each time sample (1 ms) corresponds to a different state of this layer. Each PC is randomly connected with the 80% of the GRs through the PFs, for a total of 38438 excitatory connections. Each IO is connected with one PC through one PF. Each DCN receives excitatory connections from all 100 MFs, for a total of 1200 synapses, and 2 inhibitory connections from 2 PCs, for a total of 24 synapses. The DCN-IO inhibitory input is implemented as a mechanism that decreases the IOs firing rate, induced by the incoming US, if a CR is generated before the US onset. Indeed, the noxiousness of the US diminishes if the cornea is already protected by the eyelid. The inhibition mechanism of the IOs by the DCNs translates the motor command signal into a sensory modulation, thus a single cerebellar area simultaneously tackles both motor execution and sensory prediction [15].

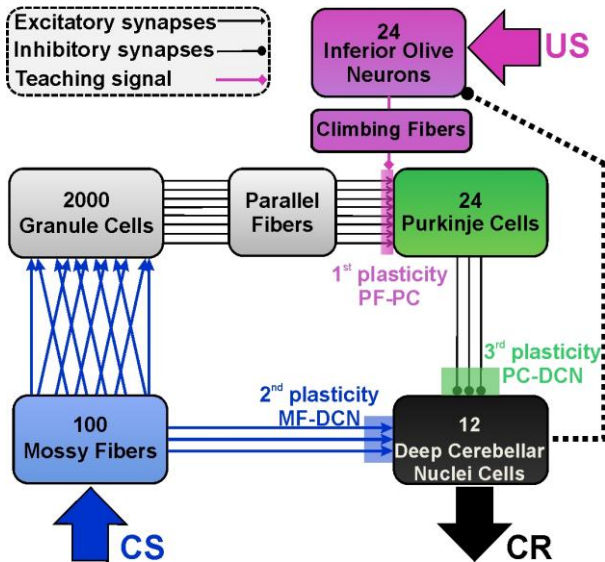


Figure 1. Cerebellar Model

Topology of the SNN models used, with connections between different groups of cells and input/output signals. Transparent areas indicate the three plasticity sites: for the one-plasticity model only the 1st plasticity is active, for the three-plasticity model also the 2nd and the 3rd plasticity are active. The inhibitory connection from DCN to IO is dashed because there is an external inhibitory mechanism.

B. Learning Rules

The SNN models embed one or three plasticity sites, which follow different learning rules:

1st learning rule: PF-PC

$$\Delta W_{PF_i \rightarrow PC_j}(t) = \begin{cases} \beta_1 \int_{-\infty}^{t_{IO\text{spike}_j}} K(t-x) \delta_{PF_i}(t-x) dx & \text{if } PC_i \text{ is active} \\ & \text{and } t = t_{IO\text{spike}_j} \\ \alpha_1 & \text{if } PC_i \text{ is active} \\ & \text{and } t \neq t_{IO\text{spike}_j} \\ 0 & \text{otherwise} \end{cases}$$

where:

$$\delta_{PF_i}(s) = \begin{cases} 1 & \text{if } PF_i \text{ is active at time } s \\ 0 & \text{otherwise} \end{cases}$$

and the Kernel function is:

$$K(z) = A \cdot e^{-\frac{z}{\tau}} (\sin(2\pi \frac{z}{\tau}))^{20}$$

where β_1 is the LTD₁ constant (= -1.0); α_1 is the LTP₁ constant (= 0.005); $t_{IO\text{spike}_j}$ is the time when the corresponding CF_j emits a spike; K is the integral kernel function, which has its peak at t_0 before $t_{IO\text{spike}_j}$ with t_0 equals to 100 ms, as the physiological delay of the neural circuit dictated by biology. τ and A are constant factor to normalize the kernel, more detailed explanations about the rationale of the kernel function can be found in [14].

2nd learning rule: MF-DCN

$$\Delta W_{MF_i \rightarrow DCN_j}(t) = \begin{cases} \beta_2 \int_{-\infty}^{+\infty} K(t-x) \delta_{MF_i}(t-x) dx & \text{if } MF_i \text{ is active} \\ & \text{and } t = t_{PC\text{spike}_j} \\ \alpha_2 & \text{if } MF_i \text{ is active} \\ & \text{and } t \neq t_{PC\text{spike}_j} \\ 0 & \text{otherwise} \end{cases}$$

where:

$$\delta_{MF_i}(s) = \begin{cases} 1 & \text{if } MF_i \text{ is active at time } s \\ 0 & \text{otherwise} \end{cases}$$

and the Kernel function is:

$$K(z) = e^{-\frac{|z|}{\tau}} (\cos(\frac{z}{\tau}))^2$$

where β_2 is the LTD₂ constant (= $-2.2 \cdot 10^{-7}$), α_2 is the LTP₂ constant (= $3.2 \cdot 10^{-6}$); $t_{PC\text{spike}_j}$ is the time when one of the two corresponding PC_j emits a spike; K is the integral kernel function and τ is used in order to normalize the arguments in the learning rule.

3rd learning rule: PC-DCN

This learning rule is implemented as a standard Spike-Timing Dependent Plasticity (STDP): when one of the two PCs (pre-synaptic) fires and soon after the corresponding DCN fires (within a pre-defined LTP-time window = 10 ms), the two inhibitory synapses from PCs to that DCN are increased, depending also on the distance between PC and DCN spikes (max LTP change: $\alpha_3 = 4.0 \cdot 10^{-4}$); otherwise, if the opposite chronological order occurs (within a pre-defined LTD-time window = 50 ms), the synapses undergo LTD (max LTD change $\beta_3 = 9.0 \cdot 10^{-6}$).

The used LTP and LTD constants for the three learning rules come from a parameter optimization as explained in [12].

C. Protocol

We used the “delayed EBCC” protocol (CS and US co-terminate) in order to test the models capability to acquire and extinguish the CRs. The protocol is divided in two sessions (session₁ and session₂), each session is composed of an acquisition phase, with the presentation of CS-US pairs for 400 trials, and an extinction phase, with the presentation of CS only for 200 trials. We used 3 different ISIs to test the robustness of the models: 300 ms (ISI₁), 400 ms (ISI₂) and 500 ms (ISI₃). The CS lasts a time equal to the sum of ISI and the duration of US (100 ms).

During the CS, the MFs randomly fire with a firing rate of about 40 Hz. During the US, IOs fire with a mean firing rate of 1 Hz and maximum firing rate of 10 Hz [10]. The DCNs spiking activity is decoded into the “cerebellar output” by a firing rate approach. A CR is identified when the cerebellar output overcomes a predefined threshold equal to 20. When a CR is identified, during the following US the IOs activity is reduced of 50%, due to the DCN-IO inhibitory loop.

D. Data Analysis

For each of the two models and for each ISI, we measured the percentage of acquired CRs during the whole test, with a mobile window of 10 trials, the Root Mean Square (RMS) cerebellar output within each trial and the latency of CRs, defined as the time difference between the US and CR onsets. We computed the mean and standard deviation for CRs percentage, RMS cerebellar output and latency, both in the acquisition phase of session₁ (trials 51-400) and in session₂ (trials 651-1000). We analyzed the synaptic weights evolution for the connection strengths modified by the learning rules: PF-PC, MF-DCN and PC-DCN.

III. RESULTS

For the one-plasticity model, the outcome is summarized in Table I.

TABLE I. ONE-PLASTICITY MODEL OUTPUT

	CRs percentage [%]	RMS output	Latency [ms]
ISI ₁ session ₁	93.2 ± 5.0	11.3 ± 1.4	173 ± 12
ISI ₁ session ₂	90.6 ± 4.1	10.5 ± 0.7	164 ± 8
ISI ₂ session ₁	91.4 ± 6.3	8.8 ± 0.6	134 ± 8
ISI ₂ session ₂	89.8 ± 4.9	8.6 ± 0.5	139 ± 5
ISI ₃ session ₁	88.1 ± 6.2	8.6 ± 0.7	129 ± 8
ISI ₃ session ₂	86.3 ± 7.2	7.9 ± 0.4	122 ± 7

It is clear that there are no significant differences between the outcomes of the model in session₂ with respect to session₁. Therefore, the single cortical plasticity could reflect a fast process and cannot consolidate the learning into more stable memory.

For the three-plasticity model the outcome is summarized in Table II.

TABLE II. THREE-PLASTICITY MODEL OUTPUT

	CRs percentage [%]	RMS output	Latency [ms]
ISI ₁ session ₁	93.7 ± 5.7	11.7 ± 1.1	166 ± 15
ISI ₁ session ₂	100.0 ± 0.0	15.8 ± 0.8	192 ± 4
ISI ₂ session ₁	93.0 ± 4.7	9.6 ± 0.8	149 ± 10
ISI ₂ session ₂	100.0 ± 0.0	13.9 ± 1.2	174 ± 8
ISI ₃ session ₁	90.3 ± 5.0	8.7 ± 0.7	123 ± 14
ISI ₃ session ₂	100.0 ± 0.0	12.3 ± 0.8	170 ± 4

Using this model, the cerebellar outcome in session₂ is higher with respect to session₁ (Fig. 2) and the latencies are greater (i.e. the CRs are more anticipated with respect to the incoming US onset). Therefore, the additional plasticity sites are supposed to consolidate the learning due to their slower dynamics. If we compare the results of the three-plasticity model with the one-plasticity model, the learning in the second session of acquisition is higher and faster in the model with multiple plasticities: in session₂ the three-plasticity model produces CRs 10 trials faster for ISI₁, 18 trials for ISI₂ and 20 trials for ISI₃ with respect to the other model. Analyzing the weights evolution along the three tests, it is possible to discover that with the multiple plasticity model there is a memory transfer from the cerebellar cortex (1st plasticity) to the deep nuclei (2nd and 3rd plasticities). It is demonstrated by the number of near low-saturated (<1 nS) weights of PF-PC synapses at the end of acquisition in session₁ (trial 400) and in session₂ (trial 1000) in Table III.

TABLE III. PERCENTAGE OF SATURATED PF-PC WEIGHTS

	1-plasticity model	3-plasticity model
ISI ₁ session ₁	20.7 %	20.5 %
ISI ₁ session ₂	21.8 %	15.3 %
ISI ₂ session ₁	17.8 %	16.9 %
ISI ₂ session ₂	18.7 %	12.9 %
ISI ₃ session ₁	18.0 %	17.1 %
ISI ₃ session ₂	18.3 %	12.6 %

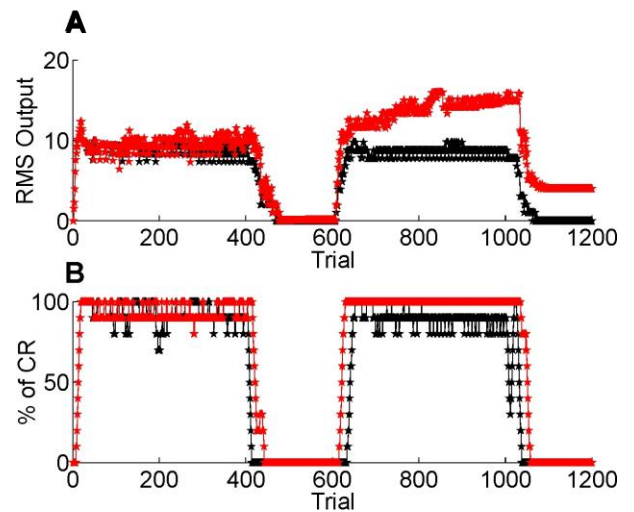


Figure 2. Cerebellar output RMS and behavioral outcome

RMS cerebellar output computed within each trial (A) and percentage of CRs (B) with ISI₂. In black the results with one-plasticity model, in red the results with three-plasticity model.

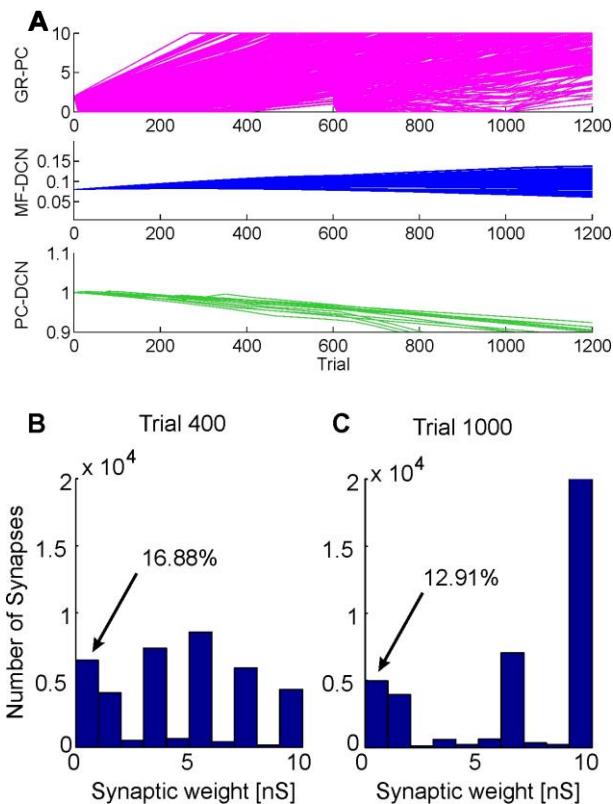


Figure 3. Synaptic weights evolution in the three plasticity sites

(A) Synaptic weights evolution with ISI_2 using the three-plasticity model. All connection weights are expressed in nS. Histograms of PC-PC weights at the end of acquisition in session₁ (B) and in session₂ (C).

It is clear that for the one-plasticity model the number of saturated PF-PC weights is about the same in both sessions, instead for the three-plasticity model the number of saturated PC-PC weights decreases from session₁ to session₂. It is due to the memory transfer: in fact the main phenomenon driving acquisition is the development of LTD at the PF-PC synapses, but in the three-plasticity model, with a slower rate, plasticity at the MF-DCN and PC-DCN synapses occurs (Fig. 3). In session₁, this transfer does not change any overall learning performances and the network is able to rapidly extinct the stimuli association by fast PF-PC LTP, without canceling the slower nuclear plastic changes occurred. Thus, session₂ controlled by the three-plasticity model starts with the cerebellar synapses in a different state than when controlled by the one-plasticity model: the distributed plasticity dynamics, able to store information, is responsible for the higher learning rate in session₂ and the more effective acquisition.

CONCLUSION

In this work, we have demonstrated that a realistic cerebellar model which embeds a distributed plasticity shows different timescales of learning and improves its performance with respect to the same model with the cortical plasticity only. Through the designed EBCC protocol, we validated the models robustness in learning associative

responses with different ISIs and we have shed light on acquisition, extinction and consolidation mechanisms, associable to the different active plasticity sites [16]. This model, eventually equipped with more realistic neuron dynamics, could represent a useful clinical tool. Indeed, the SNN with modified parameters so as to reproduce cerebellar abnormalities, such as lesions or cellular disruption, could predict the expected and correlated behavioral outcomes. On the other hand, by fitting the model on specific patients' misbehaviors, it could suggest the underlying parameters modifications.

REFERENCES

- [1] R. B. Ivry and J. V. Baldo, "Is the cerebellum involved in learning and cognition?," *Curr. Opin. Neurobiol.*, vol. 2, no. 2, pp. 212–6, Apr. 1992.
- [2] R. F. Thompson, "Neural mechanisms of classical conditioning in mammals," *Philos. Trans. R. Soc. London. Ser. B Biol. Sci.*, vol. 329, no. 1253, pp. 161–170, Aug. 1990.
- [3] J. F. Medina and M. D. Mauk, "Computer simulation of cerebellar information processing," *Nat. Neurosci.*, vol. 3 Suppl, no. SUPPL., pp. 1205–11, Nov. 2000.
- [4] M. Ito, "Cerebellar microcomplexes," *Int. Rev. Neurobiol.*, vol. 41, pp. 475–87, Jan. 1997.
- [5] C. Hansel, D. J. Linden, and E. D'Angelo, "Beyond parallel fiber LTD: the diversity of synaptic and non-synaptic plasticity in the cerebellum," *Nat. Neurosci.*, vol. 4, no. 5, pp. 467–75, May 2001.
- [6] E. D'Angelo, S. K. E. Koekkoek, P. Lombardo, S. Solinas, E. Ros, J. A. Garrido, M. Schonewille, and C. I. De Zeeuw, "Timing in the cerebellum: oscillations and resonance in the granular layer," *Neuroscience*, vol. 162, no. 3, pp. 805–15, Sep. 2009.
- [7] J. Monaco, C. Casellato, G. Koch, and E. D'Angelo, "Cerebellar theta burst stimulation dissociates memory components in eyeblink classical conditioning," *Eur. J. Neurosci.*, no. July, pp. 1–8, Sep. 2014.
- [8] C. Casellato, A. Antonietti, J. A. Garrido, A. Pedrocchi, and E. D'Angelo, "Distributed cerebellar plasticity implements multiple-scale memory components of Vestibulo-Ocular Reflex in real-robots," in *5th IEEE RAS/EMBS International Conference on Biomedical Robotics and Biomechanics*, 2014, pp. 813–818.
- [9] J. A. Garrido, N. R. Luque, E. D'Angelo, and E. Ros, "Distributed cerebellar plasticity implements adaptable gain control in a manipulation task: a closed-loop robotic simulation," *Front. Neural Circuits*, vol. 7, no. October, p. 159, Jan. 2013.
- [10] R. R. Carrillo, E. Ros, C. Boucheny, and O. J. M. D. Coenen, "A real-time spiking cerebellum model for learning robot control," *Biosystems*, vol. 94, no. 1, pp. 18–27, 2008.
- [11] T. Yamazaki and J. Igarashi, "Realtime cerebellum: A large-scale spiking network model of the cerebellum that runs in realtime using a graphics processing unit," *Neural Networks*, vol. 47, pp. 103–111, Nov. 2013.
- [12] C. Casellato, A. Antonietti, J. A. Garrido, R. R. Carrillo, N. R. Luque, E. Ros, A. Pedrocchi, and E. D'Angelo, "Adaptive Robotic Control Driven by a Versatile Spiking Cerebellar Network," *PLoS One*, vol. 9, no. 11, p. e112265, Nov. 2014.
- [13] J. F. Medina, K. S. Garcia, and M. D. Mauk, "A mechanism for savings in the cerebellum," *J. Neurosci.*, vol. 21, no. 11, pp. 4081–4089, 2001.
- [14] E. Ros, R. R. Carrillo, E. M. Ortigosa, B. Barbour, and R. Agis, "Event-driven simulation scheme for spiking neural networks using lookup tables to characterize neuronal dynamics," *Neural Comput.*, vol. 18, no. 12, pp. 2959–93, Dec. 2006.
- [15] I. Herreros and P. F. M. J. Verschure, "Nucleo-olivary inhibition balances the interaction between the reactive and adaptive layers in motor control," *Neural Networks*, vol. 47, pp. 64–71, 2013.
- [16] E. D'Angelo, S. Solinas, J. A. Garrido, C. Casellato, A. Pedrocchi, J. Mapelli, D. Gandolfi, and F. Prestori, "Realistic modeling of neurons and networks: towards brain simulation," *Funct. Neurol.*, vol. 28, no. 3, pp. 153–166, 2013.